Improving the Performance of Saturated Cores Fault Current Limiters by Varying Winding Density in the AC Coils

Y. Nikulshin, Y. Wolfus, A. Friedman, and Y. Yeshurun

***Abstract*—Effect of the winding density in the AC coils on the performance of a saturated cores fault current limiter (SCFCL) has been studied, exploiting Finite Element Analysis. For a given design, a fixed number of turns was concentrated at the center of the AC coils limb, resulting in high windings density. The coil length was then increased gradually along the limb, decreasing the winding density and therefore decreasing the coil impedance. However, we found that the ratio between the fault to nominal state impedances increases with decreasing winding density. The results are discussed and explained as originating from the change in the flux linkage of windings in the coil for various core states. In the nominal-state of the SCFCL, the core is saturated and the coupling between the windings is lower, given the lower winding density. However, when the core is desaturated during a fault, the magnetic interaction of the windings with the core strengthens, the coupling between the windings increases and contributes to higher fault-state impedance. Thus, reducing the winding density may serve in increasing the impedance ratio of the device and improving the performance of SCFCLs. The results suggest that the windings density in SCFCLs should be used as a significant design parameter.**

***Index Terms*—Coil impedance, core saturation, finite elements analysis, saturated cores fault current limiter.**

I. Introduction

THE continuous growth of energy generation and the worldwide effort to integrate renewable energy sources in existing grids result in a need to solve the problem of fault currents [1]–[4]. Recent R&D projects aiming at developing fault current limiter (FCL) solutions have led to several device demonstrators installed in power facilities [5]–[7].

The saturated cores fault current limiter (SCFCL) is one of the promising concepts for limiting fault currents in distribution and transmission level grids. The SCFCL utilizes a complex magnetic circuit composed of several coils sharing common magnetic cores: AC coils are connected in series to the grid and DC coils are configured to saturate the core. The operation principle of SCFCL was described in several papers [8]–[11]. The SCFCL is characterized by two principal parameters: impedance at nominal current (insertion impedance) and impedance at fault current (limiting impedance). The impedance is mostly reactive, being defined by the sum of the inductances of the AC coils.

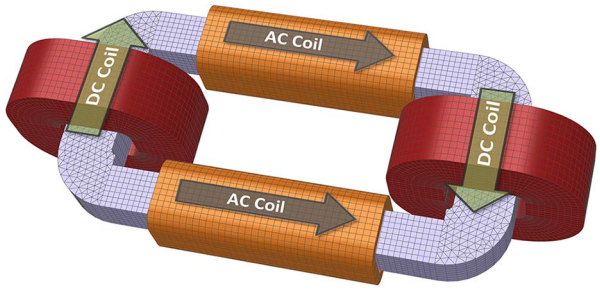

Fig. 1. 3D model of SCFCL utilizing one magnetic core, two AC coils in series in the same direction and two DC coils for magnetic bias.

The inductance of each of the AC coils depends on the permeability of the magnetic core which varies along the core limb; the permeability is current dependent and hence time dependent. The minimal value of the insertion impedance is limited by the air inductance (at 100% saturation of the core) of the AC coil. In an air core coil, the flux linkage between each winding of the coil is determined only by the distance between the windings. However, for a nonlinear magnetic core, flux linkage and overall inductance depend on the spatial and current dependent core state.

In this paper we describe a study of SCFCL with different AC coil lengths in various regimes. We focus on one promising, compact and material saving closed core design [12] and study the effect of the AC coils length on the SCFCL behavior. For such a system, traditional methods of magnetic circuit design are incompatible. For calculating the current dependent inductance, $L(I)$, of the AC coils we exploited through Finite Element Method (FEM) using COBHAM Opera software package and Matlab. Simulations of performance of this model are compared with measurements of a laboratory scale model with constant coil length. The method for extracting $L(I)$ and its use for predicting the full voltage waveform at any given operating conditions is described in a previous work [15].

II. Experimental

Fig. 1 exhibits the single phase SCFCL studied in this work. This design uses a single magnetic core. Two bias DC coils, forming a closed DC magnetic circuit, are mounted on the

Manuscript received August 12, 2014; accepted November 25, 2014. Date of current version March 20, 2015. This work was supported in part by the Israeli Ministry of Energy and Water.

The authors are with the Institute of Superconductivity, Department of Physics, Bar-Ilan University, Ramat-Gan 52900, Israel (e-mail: yasha.nick@gmail.com).

Color versions of one or more of the figures in this paper are available online at http://ieeexplore.ieee.org.

Digital Object Identifier 10.1109/TASC.2014.2386323

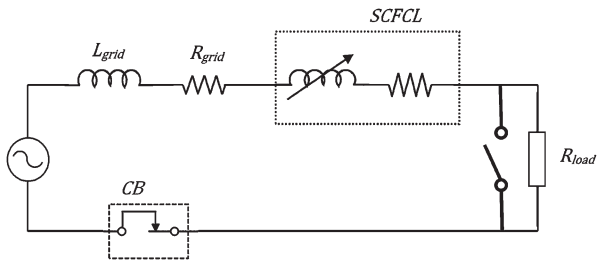

Fig. 2. Electric grid with SCFCL.

TABLE I
PARAMETERS OF LABORATORY AC GRID

Parameter	Value
Voltage RMS [V]	230
Frequency [Hz]	50
Grid inductance, $L_{\rm grid}$ [mH]	4.5
Grid resistivity, $R_{\rm grid}$ [Ω]	0.48
Normal load [Ω]	35.2
Overload [Ω]	18

core's short limbs. AC coils are mounted on the long limbs generating magnetic flux in the same direction. Clearly, the AC coil magnetic circuit is open.

The SCFCL is characterized by its resistive and inductive components of impedance when installed in a grid: $R_{\rm grid}$ and $L_{\rm grid}$. Fig. 2 shows schematics of the electrical circuit.

The differential equation describing the voltage in the above circuit is given by:

$$V\cos(\omega t) = I(R_{\rm load} + R_{\rm grid} + R_{fcl}) + L_{\rm grid}\frac{dI}{dt} + \frac{d}{dt}(L_{\rm fcl}I) \tag{1}$$

where L and R are the inductance and resistance of the circuit elements, and I is the current. The voltage may also be presented as a function of the time dependent current $I(t)$:

$$V\cos(\omega t) = I(R_{\rm load} + R_{\rm grid} + R_{\rm fcl}) + \frac{dI}{dt}\left(L_{\rm grid} + L_{\rm fcl}(I) + I\frac{dL_{\rm fcl}}{dI}\right). \tag{2}$$

To solve this equation it is necessary to know the current dependence of the SCFCL inductance $L_{\rm fcl}$ which strongly depends on the core magnetic state. In [15] we demonstrated methods for finding the curves $L_{\rm fcl}(I)$ experimentally and by FEM simulations, both providing similar results. Using such methods for extracting the $L_{\rm fcl}(I)$ curve for an SCFCL with one variable parameter allows studying the effect of this parameter on the SCFCL when installed in the grid. In this work we study the effect of AC coils length on the SCFCL behavior in electric grid.

Parameters of the grid and SCFCL are listed in Tables I and II correspondingly. $L_{\rm fcl}(I)$ curves have been obtained by using the simulations method. For simplicity $L(I)$ is used instead of $L_{\rm fcl}(I)$ for the rest of this work.

TABLE II
PARAMETERS OF SCFCL

FCL element	Parameter	Value
Core	AC limb length, mm	300
	AC limb cross-section, mm^2	40x40
	DC limb cross-section, mm^2	50x40
AC coil	Length, mm	variable
	Turns, number	148
DC coil	Turns, number	200
	Current, Ampere	43
	DC limb length, mm	200

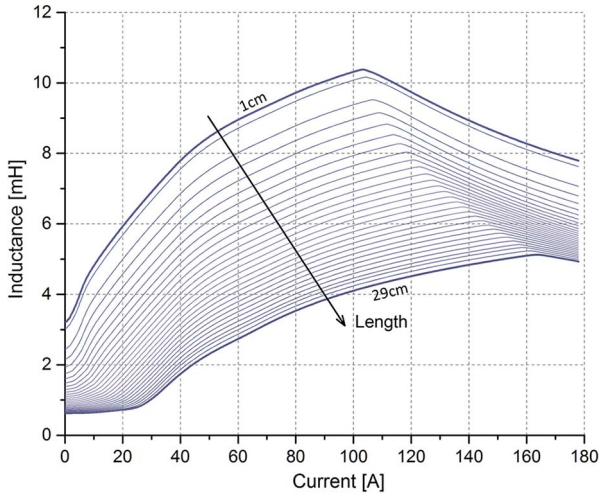

Fig. 3. $L_{\rm fcl}(I)$ curves of SCFCL models with varying AC coil lengths. Arrow denotes the direction of increasing coil length from 1 cm (top curve) to 29 cm (bottom).

III. RESULTS AND DISCUSSION

29 transient FEM simulations for AC coil lengths varying from 1 to 29 cm have been performed. The number of turns is kept constant hence different coil lengths translate to different "winding density" in the coil. $L(I)$ curves obtained by this method are shown in Fig. 3. Typically, $L(I)$ is non-monotonic and nonlinear. For a given coil length, the lowest value of L is obtained for zero AC current, when the core section under the coil is saturated to its highest possible level. L increases with increasing coil current and reaches a maximal value after which further increase in current leads to decrease in L. The maximum of L reflects the current level for which the core magnetization is at its lowest value and permeability is maximal. Higher current values result in core regions entering a reversed saturation state and hence lower L values [13].

The arrow in Fig. 3 marks the direction of increasing coil length (decreasing winding density). The top curve exhibits $L(I)$ of the shortest coil (1 cm) mounted at the center of the limb. Since the "weakest" saturation level along the core limb is obtained at its center, the $L(I)$ curve for the shortest coil exhibits the highest zero current inductance. Having a short dense coil situated at the center of the limb easily desaturates the core limb, consequently the $L(I)$ curve begins its ascending in accordance to low current values and reaches top values compared to longer coils. The bottom $L(I)$ curve corresponds to the longest coil (29 cm). Here initial inductance is reduced due

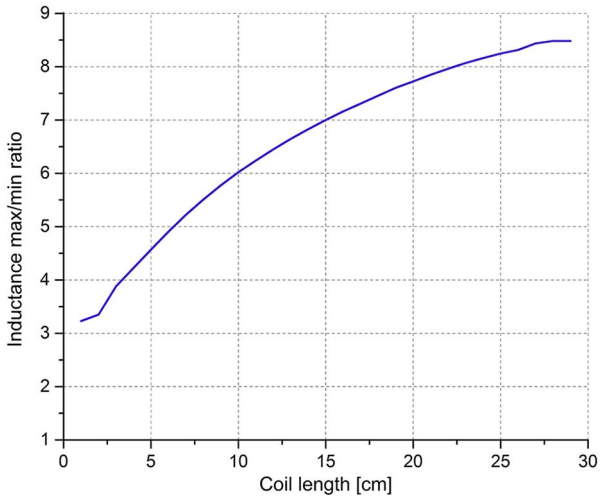

Fig. 4. The ratio between highest and lowest inductance values.

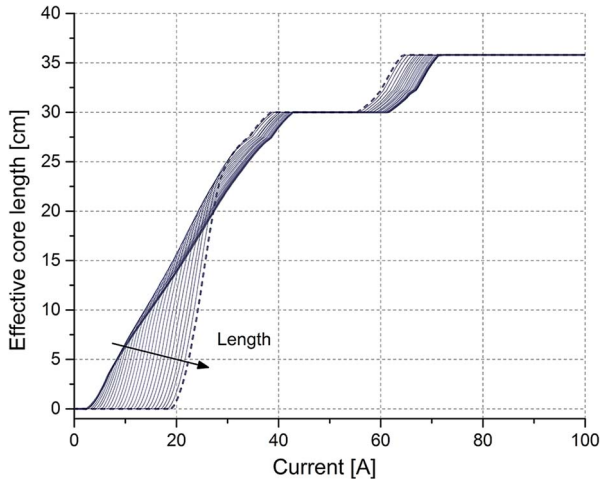

Fig. 5. Dependence of the effective core length (ECL) on AC coils current. Arrow marks the direction of increasing coil length (1 to 29 cm).

to better average saturation of the core section under the coil. Desaturation is pushed to higher currents and the maximum in L is reduced. In general, it is evident from Fig. 3 that both the insertion and maximal inductance decrease with increasing coil length and that the maximal inductance is pushed to higher current values.

One of the most important parameters characterizing the SCFCL in the grid is its impedance ratio between fault to nominal operating states. Higher impedance ratio means a more flexible device, which serves better for installation in the grid. Fig. 4 displays the maximal to minimal inductance ratio, extracted from Fig. 3, as a function of coil length. This ratio increases with increasing coil length in a nonlinear manner and reaches maxima at the full length of the limb. This result implies that the rate at which $\mathrm{L_{min}}$ decreases with increasing length exceeds that of $\mathrm{L_{max}}$ decreases with increasing length. To explain this result one should consider the mutual inductance between the windings in the coil as well as the nonlinear nature of the magnetic core. When the core is saturated, longer coils, lower winding density coils, exhibit lower coupling between windings and higher flux leakage is obtained in comparison with short dense coils. However, when the core is desaturated, its permeability sharply increases and the coupling between coil windings strengthens. As a result, the relative drop in the coil maximal inductance for long coils is smaller than the drop in its minimal inductance. This result suggests that SCFCLs with longer AC coils (lower winding density) exhibits higher inductance change and may be more adequate for some grid installations.

In [14] the concept of effective core length was introduced and defined as the length of the non-saturated part of the core. By measuring this length for different coils we can analyze the dynamics of the desaturation process.

Fig. 5 shows the effective core length (ECL) as a function of the AC coil current for different coil lengths. The arrow marks the direction of increasing coil length. For short coils ECL begins its increase already at very low currents. ECL for the shortest coil (1 cm) grows gradually in the current interval of 3.5 A to 42 A while for the 29 cm coil this current interval narrows and is observed from 19.5 A to 38 A. The first plateau in ECL is observed when ECL reaches the full length of the AC limb. When the AC current further increases, it drives the core section under the DC coils out of saturation and a second step and plateau are obtained in ECL. As is evident from Fig. 5, the second step in ECL is observed at lower currents for longer coil lengths and this is a result of the coil windings stretching to closer vicinity to the DC coil.

The DC magnetization can also be adjusted for improving SCFCL performance. When core desaturation pushed to higher currents it maintains a low insertion impedance for a higher nominal current up to 19.5 A. A steeper slope of ECL-current dependence means that the SCFCL changes its inductance faster, leading to a larger contribution of the dL/dt term of equation (1) hence, higher voltage drop on the SCFCL and better first current peak limiting. In Fig. 6 the flux density distribution along the core axis is presented for 1, 9, 19, 29 cm coil lengths at the very beginning of the desaturation process. The current at this point is different for every coil. The magnetic flux density B reaches the same value at the middle point of the core (0 cm) but the profiles along the axis are different. For short coils the B profile exhibits a narrow well form and it expands towards the edges of the core with increasing current. For the 1 cm coil the core section beneath the coil is fully desaturated, the inductance continues to grow with current due to growing ECL and the decreasing internal demagnetization factor [15]. For the 29 cm coil at 20 A almost the entire core is desaturated leading to larger inductance change. For maximum fault/nominal impedance ratio rapid ECL growth is required.

The RMS values of the insertion impedance and short circuit limited current are of importance for practical use of SCFCLs. Also of interest is the voltage drop across the SCFCL terminals at nominal and limited fault currents. These values can be calculated by solving equation (1) at different conditions. Fig. 7 displays the non-sinusoidal waveform of voltage drop on SCFCL obtained by solving the equation utilizing $L(I)$ curves described in Fig. 3. The limited current is not a pure sinus and has higher harmonics in its waveform. The prospective current remains sinusoidal due to linear components of the grid.

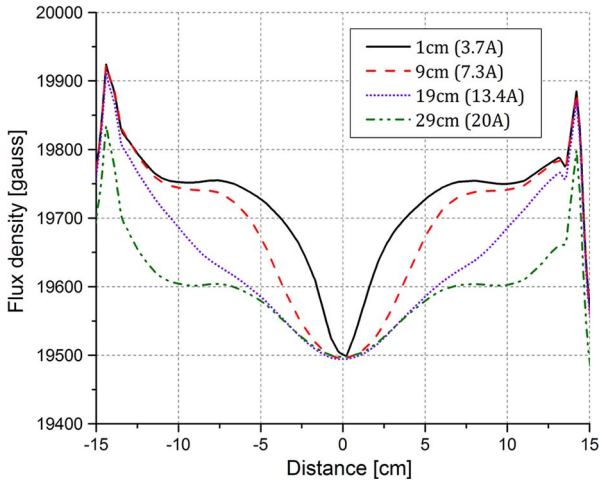

Fig. 6. Magnetic flux density distribution along the core length at the start of desaturation.

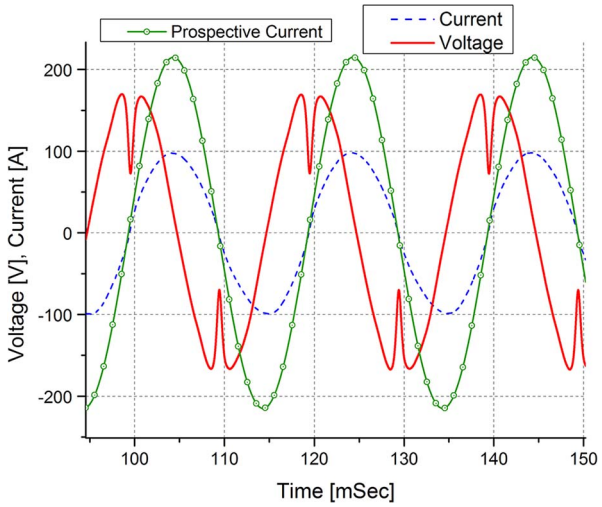

Fig. 7. Voltage drop (solid red) on SCFCL, limited current (dashed blue) and prospective current (solid green) obtained for a 20 cm long coil.

For practical use of the SCFCL in the grid, it is useful to describe its performances in terms of its RMS current, voltage and impedance values. Fig. 8(a) displays the RMS voltage curves as a function of the RMS current for different coil lengths. Fig. 8(b) displays the impedance defined as $V_{\rm rms}/I_{\rm rms}$. RMS values are extracted from the actual waveforms as displayed in Fig. 8.

For proving the simulation results for the laboratory scale SCFCL model with a 20 cm AC coil we have measured impedance values lower than 0.3 Ohm for currents up to 11.5 $A_{\rm rms}$. With the increase in current up to 105 $A_{\rm rms}$ we observed an increase in impedance to 1.85 Ohm namely, impedance increases 6 folds from nominal to fault states. This model was tested in a grid of 230 $V_{\rm rms}$, nominal current of about 6.5 $A_{\rm rms}$ and prospective short circuit current of 154.5 $A_{\rm rms}$. The voltage drop on the SCFCL showed 0.77% for nominal current, less than the typical 1% insertion impedance requirement. Detailed measurement procedure is described in [15]. During fault, the

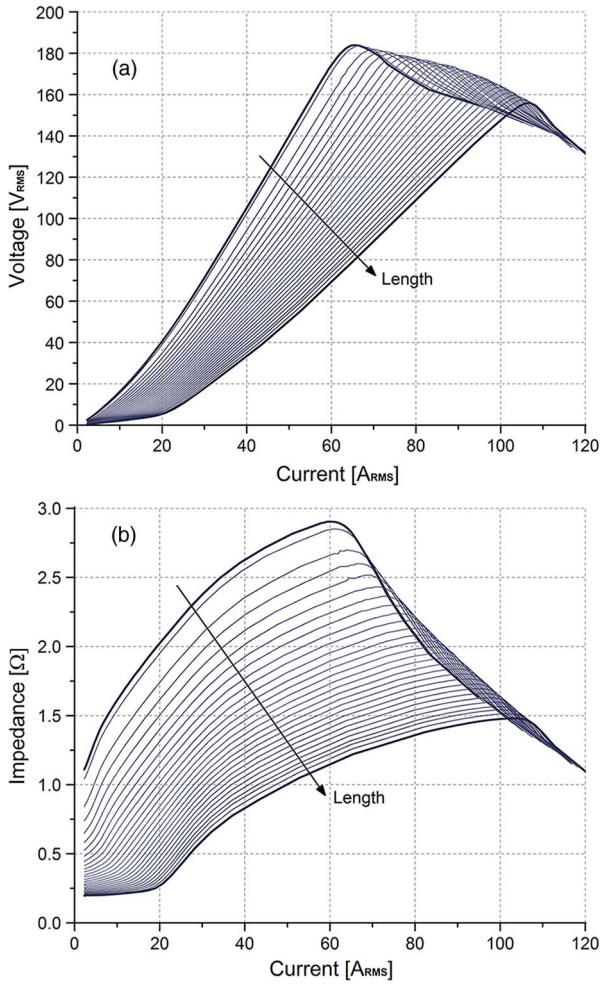

Fig. 8. (a) Current dependence of impedance and (b) voltage drop on SCFCL of considered SCFCL model with AC coil lengths of 1 to 29 cm.

voltage drop becomes significant part of total grid voltage. Short circuit current depends not only on SCFCL characteristic but also on the grid parameters. For the grid configuration used here a limited short circuit current of 74.5 $A_{\rm rms}$ has been obtained namely, fault current limiting of about 50%.

IV. Conclusion

The effect of AC coil length and its winding density has been investigated. It was shown that winding density affects the performances of the saturated cores FCL and the ratio between the fault to the normal state impedances increases with reducing winding density for a fixed number of turns. This result is explained by the nonlinear core magnetization effect on the mutual inductance between windings in the AC coil. For a deeply saturated core, flux linkage between the windings causes the mutual inductance to decrease for a lower winding density. However, when the core is desaturated, it recouples the windings, and mutual inductance increases. It was shown that mutual windings' inductance may serve as an additional degree of freedom in the design of saturated cores FCL and that a variation of such design parameter may be realized by varying the winding density in the AC coils.

REFERENCES

[1] M. Noe, M. Steurer, S. Member, S. Eckroad, and R. Adapa, "Progress on the R&D of fault current limiters for utility applications," in *Proc. IEEE Power Energy Soc. Gen. Meet.*, 2008, pp. 1–4.

[2] O. Naeckel and M. Noe, "Design and test of an air coil superconducting fault current limiter demonstrator," *IEEE Trans. Appl. Supercond.*, vol. 24, no. 3, pp. 1–5, Jun. 2014.

[3] D. Cvoric, S. W. H. de Haan, and J. A. Ferreira, "Comparison of the four configurations of the inductive fault current limiter," in *Proc. IEEE Power Electron. Spec. Conf.*, Jun. 2008, pp. 3967–3973.

[4] F. Moriconi and F. D. La Rosa, "Development and deployment of saturated-core fault current limiters in distribution and transmission substations," *IEEE Trans. Appl. Supercond.*, vol. 21, no. 3, pp. 1288–1293, Jun. 2011.

[5] J. Bock *et al.*, "HTS fault current limiters—First commercial devices for distribution level grids in Europe," *IEEE Trans. Appl. Supercond.*, vol. 21, no. 3, pp. 1202–1205, Jun. 2011.

[6] J. Moscrop and F. Darmann, "Design and development of a 3-phase saturated core high temperature superconducting fault current limiter," in *Proc. Int. Conf. EPECS*, 2009, pp. 1–6.

[7] B. Raju, K. Parton, and T. Bartram, "A current limiting device using superconducting dc bias applications and prospects," *IEEE Trans. Power App. Syst.*, vol. PAS-101, no. 9, pp. 3173–3177, Sep. 1982.

[8] V. Rozenshtein *et al.*, "Saturated cores FCL—A new approach," *IEEE Trans. Appl. Supercond.*, vol. 17, no. 2, pp. 1756–1759, Jun. 2007.

[9] Y. Wolfus, Y. Yeshurun, A. Friedman, V. Rozenstein, and Z. Bar-Haim, "Fault current limiter with saturated core," U.S. Patent Appl. US2012/0154966 A1, Aug. 31, 2010.

[10] L. Martini *et al.*, "Resistive fault current limiter prototypes: Mechanical and electrical analyses," *J. Phys. Conf. Ser.*, vol. 43, pp. 925–928, Jun. 2006.

[11] S. Wolfus, Y. Yeshurun, A. Friedman, V. Rozenshtein, and Z. Bar-Haim, "Fault current limiters (FCL) with the cores saturated by superconducting coils," U.S. Patent US8 351 167, Jan. 8, 2013.

[12] Y. Nikulshin and A. Friedman, "Dynamic desaturation process in saturated cores fault current limiters," *IEEE Trans. Appl. Supercond.*, vol. 22, no. 3, Jun. 2012, Art. ID. 5601704.

[13] Y. Nikulshin, Y. Wolfus, A. Friedman, and Y. Yeshurun, "Dynamic core length in saturated core fault current limiters," *Supercond. Sci. Technol.*, vol. 26, no. 9, Sep. 2013, Art. ID. 095013.

[14] E. Pardo and A. Sanchez, "Demagnetizing factors of rectangular prisms and ellipsoids," *IEEE Trans. Magn.*, vol. 38, no. 4, pp. 1742–1752, Jul. 2002.

[15] Y. Nikulshin, Y. Wolfus, A. Friedman, and Y. Yeshurun, "Dynamic inductance in saturated cores fault current limiters," *J. Supercond. Novel Magn.*, vol. 28, no. 2, pp. 579–583, Sep. 2014.